THE JOURNAL OF PHYSICAL CHEMISTRY B
A JOURNAL OF THE AMERICAN CHEMICAL SOCIETY

pubs.acs.org/JPCB

Article

Long Vibrational Lifetime R-Selenocyanate Probes for Ultrafast Infrared Spectroscopy: Properties and Synthesis

Sebastian M. Fica-Contreras, Robert Daniels, Omer Yassin, David J. Hoffman, Junkun Pan, Gregory Sotzing,* and Michael D. Fayer*

Cite This: *J. Phys. Chem. B* 2021, 125, 8907−8918

Read Online

ACCESS | Metrics & More | Article Recommendations | Supporting Information

ABSTRACT: Ultrafast infrared vibrational spectroscopy is widely used for the investigation of dynamics in systems from water to model membranes. Because the experimental observation window is limited to a few times the probe's vibrational lifetime, a frequent obstacle for the measurement of a broad time range is short molecular vibrational lifetimes (typically a few to tens of picoseconds). Five new long-lifetime aromatic selenocyanate vibrational probes have been synthesized and their vibrational properties characterized. These probes are compared to commercial phenyl selenocyanate. The vibrational lifetimes range between ∼400 and 500 ps in complex solvents, which are some of the longest room-temperature vibrational lifetimes reported to date. In contrast to vibrations that are long-lived in simple solvents such as CCl_4, but become much shorter in complex solvents, the probes discussed here have ∼400 ps lifetimes in complex solvents and even longer in simple solvents. One of them has a remarkable lifetime of 1235 ps in CCl_4. These probes have a range of molecular sizes and geometries that can make them useful for placement into different complex materials due to steric reasons, and some of them have functionalities that enable their synthetic incorporation into larger molecules, such as industrial polymers. We investigated the effect of a range of electron-donating and electron-withdrawing *para*-substituents on the vibrational properties of the CN stretch. The probes have a solvent-independent linear relationship to the Hammett substituent parameter when evaluated with respect to the CN vibrational frequency and the ipso ^{13}C NMR chemical shift.

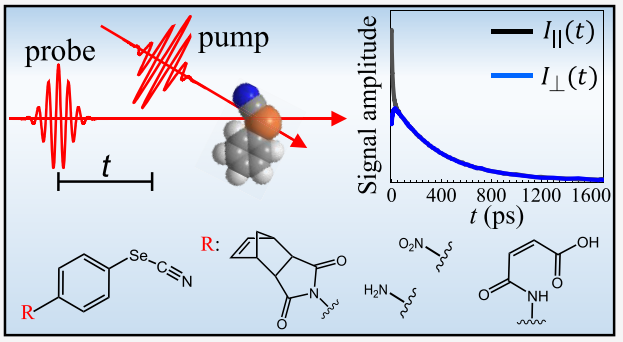

I. INTRODUCTION

Important properties of chemical systems, from water to polymers, are determined by their molecular level dynamics.[1,2] Ultrafast time-resolved IR spectroscopy is particularly well-suited for investigating the relationships among dynamics, interactions, and structures because it can measure properties such as orientational relaxation[2−5] and spectral diffusion[6−10] of a vibrational probe molecule. Such measurements can be used to investigate dynamics and how they are influenced by local and mesoscopic environments.[1,5,8,9,11−15] A successful experiment requires the detection of a spectrally resolved vibrational signal, ideally from a vibration with a lifetime at least as long as the dynamics of interest.[1,16] However, the native structures of many chemical systems suffer from overlapping signals and short vibrational lifetimes,[1,17] which are frequently not sufficient to fully capture the time range of the dynamic processes of interest.

These challenges have been circumvented by using vibrational probes. Vibrational probes are molecules that absorb infrared (IR) light, typically in the mid-IR region.[1,8−11] Their use became common practice in pump−probe and 2D IR spectroscopy, as it is possible to find probes with a spectrally resolved resonance that offers a sufficiently long vibrational lifetime. An additional desirable characteristic of vibrational probes is sensitivity to local environments, which makes it possible to investigate structural dynamics.[11] Commonly used vibrational probes include carbon−deuterium (C−D) and oxygen−deuterium (O−D) bonds,[1,12,18] nitriles (CN),[19−23] thiocyanates (SCN),[10,15,24] selenocyanates (SeCN),[16] alkynes (CC),[25] isonitriles (NCN),[26] cyanamides (NCN),[1,23,27] metal carbonyls ($M(CO)_x$),[6,28] and azides (N_3).[1,27] These groups have been used in a wide variety of applications, some of which include the replacement of native bonds with negligible structural disturbance,[8,12] the study of hydrogen bond networks,[13] molecular dynamics in proteins,[9,19,29,30] nucleic acids,[14] polymers,[5] phospholipids,[31] glasses,[32] and ionic liquids.[8,33,34] The development of new

Received: June 4, 2021
Revised: July 12, 2021
Published: August 2, 2021

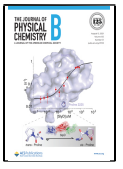

vibrational probes is an active area of research, as there is no single probe well-suited to study all chemical systems. As more vibrational probes are developed, systems of increasing structural and dynamic complexity can be studied.

Complex molecular systems, such as model biological membranes or polymers below their glass transition temperature, can have molecular level dynamics that span a wide range of time scales. At room temperature, the lifetimes of commonly used vibrations range from single-digit picoseconds to several tens of picoseconds.[1,7,9,11,12,19,26] Because the vibrational lifetime determines the experimental observation window,[16] it is not possible to use many vibrational probes to characterize a wide range of dynamic processes, for example, from 100 fs to 1 ns.

Some vibrational lifetimes have been extended by isotopic labeling and others by cryogenic cooling.[28,35,36] However, these methods are costly or do not offer realistic conditions for the study of most native molecular behaviors. Another well-documented method that lengthens vibrational lifetimes is the introduction of a heavy atom (such as S, Se, or Sn) between the probe moiety and the rest of the molecule.[16,24,30] The heavy atom isolates the vibration of the reporting vibrational mode from the high density of vibrational energy-accepting states in the rest of the molecule, causing a retardation of intramolecular vibrational relaxation and the extension of the excited state lifetime.[16,25,37] This method has been used with alkynes,[25] azides,[27] nitriles,[24] and modified amino acids.[7,16]

In addition to temporal resolution, vibrational probes provide structural resolution through solvatochromism.[11,38,39] Solvatochromism results in a vibrational frequency shift that is proportional to the magnitude of the electric field applied by the local environment along the molecule's vibrational ground and excited state dipole difference vector.[11,38,40−42] The electric field sensitivity is quantified by the Stark tuning rate (STR).[42] The ability to obtain information reported by different subensembles of spectrally resolvable vibrational probes can enable the extraction of quantitative, environment-specific, structural and dynamic information in a single chemical matrix.[11]

Nitrile probes display a single well-dispersed absorption spectrum and have relatively long lifetimes, useful molar extinction coefficients, and high STRs of up to ∼7 cm^{-1}/(GV/m).[1,9,11,39,42,43] Moreover, it has been shown that the vibrational Stark effect can account for the solvatochromism in nitriles, which simplifies the analysis of environment-specific dynamics.[42] These characteristics make nitrile probes versatile molecular reporters.[9,19] The commercially available molecule phenyl selenocyanate (PhenylSeCN) belongs to the family of nitrile probes and was found to have an extremely long vibrational lifetime of 377 ps in dimethylformamide (DMF) at room temperature. PhenylSeCN has been used to measure molecular dynamics over a large experimental observation window from ∼100 fs to ∼1 ns in amorphous glass-forming polymers.[5]

Here, we report five new long-lived selenocyanate vibrational probes. The lifetimes of the new probes and PhenylSeCN were measured in two complex solvents—dimethylformamide (DMF) and dimethyl sulfoxide (DMSO)—at room temperature, and two of the probes' lifetimes were also measured in simple solvents—carbon tetrachloride (CCl_4) and chloroform ($CHCl_3$)—and compared to the metal carbonyl, $W(CO)_6$, which in CCl_4, to our knowledge, has the longest previously reported vibrational lifetime (700 ps) at room temperature.[44] In addition, the spectral shifts of each probe were measured in up to 10 solvents, and by using this information, we investigated the probes' sensitivity to the chemical environment. All novel probes behaved essentially the same as PhenylSeCN with a Stark tuning rate (STR) of 12.3 ± 2.4 cm^{-1}/(GV/m)).[5] This STR represents an ∼2-fold increase over the typical STRs of other nitrile vibrational probes.[42] In contrast to the commercially available PhenylSeCN, which is a hydrogen bond acceptor, three of the probes are both H-bond donors and acceptors. Two of the probes have functional groups, an amine and a carboxylic acid, which can be used to synthetically attach the probes to other molecules. Four of the probes, which can be viewed as PhenylSeCN with a *para* substituent of varying electron-donating and -withdrawing strengths, were selected to investigate the substituents' electronic effects on the CN moiety. These molecules were found to have a linear relationship to the *p*-Hammett substituent parameter when evaluated with respect to the CN vibrational resonance frequency and the ipso ^{13}C nuclear magnetic resonance spectroscopy chemical shift.

The five new -SeCN probes are (*Z*)-3-(4-selenocyanatophenylcarbamoyl)acrylic acid (Acrylic AcidSeCN), norbornene dicarboximide−phenyl selenocyanate (NorborneneSeCN), *p*-nitrophenyl selenocyanate (NitroSeCN), *p*-aniline selenocyanate (AnilineSeCN), and 3-indole selenocyanate (IndoleSeCN). Schemes of the synthesis of the probes are given in Section IV, and the probes' chemical structures are shown in Figure 1. The full synthetic procedures are presented

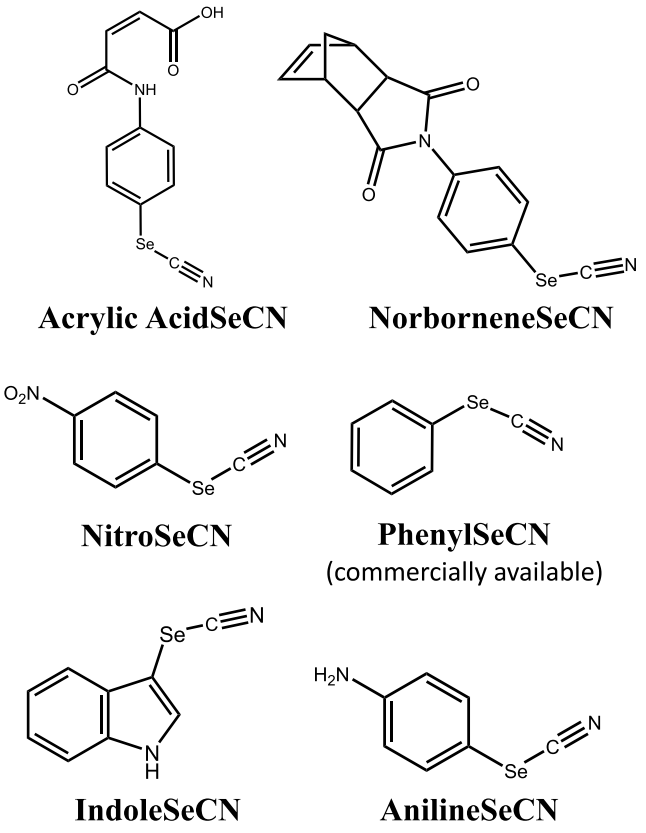

Figure 1. Chemical structures of long-lived selenocyanate vibrational probes.

https://doi.org/10.1021/acs.jpcb.1c04939
J. Phys. Chem. B 2021, 125, 8907−8918

for the five new probes in the Supporting Information. Apart from NitroSeCN, selenocyanation was achieved by addition of an electron-rich aromatic directly to triselenocyanide, which was generated by the reaction of selenium dioxide and malononitrile.[45] While this method is preferable due to its speed, simplicity, and high efficiency, its use is limited to electron-rich nitrogen- or oxygen-containing heterocycles and fails to react when using electron-poor alternatives. Therefore, for the synthesis of NitroSeCN, selenocyanation was achieved by the addition of potassium selenocyanate to an activated diazonium salt.[46]

Indole was selected as a probe for its widespread use in medical applications and ease of selenocyanation.[47] In addition, the probes were designed to fit structures commonly found in polymers such as amide−acids, imides, amines, and norbornenes to examine their potential incorporation into polymers of similar chemical structures. Such incorporations would result in the study of complex chemical systems with almost native vibrational probes, which would eliminate disturbances to the systems' native molecular behavior while still retaining the ability to study dynamics over long time scales.

The vibrational lifetimes of the probes, measured in DMF and DMSO, were hundreds of picoseconds long, which are possibly the longest vibrational lifetimes in complex environments at room temperature. In DMSO, IndoleSeCN displayed the longest lifetime (506 ps). Additionally, the lifetimes of PhenylSeCN and AnilineSeCN in two structurally simple solvents—CCl_4 and $CHCl_3$—displayed remarkable lifetimes between 730 and 1235 ps. A heuristic discussion is provided to illustrate the structural considerations that play a role in the vibrational relaxation process of these molecules.

As ultrafast vibrational experiments can typically be conducted to 4 or 5 lifetimes, these probes permit dynamics to be observed to ∼2 ns. These long lifetimes and high environmental sensitivity probes are especially well-suited for the study of structurally complex systems with highly heterogeneous environments and slow components of structural dynamics.

II. METHODS

IIA. Sample Preparation. Each vibrational probe was dissolved in a minimal volume of solvent, and a few drops of the resulting solution were deposited between two calcium fluoride (CaF_2) windows, separated by a 250 μm Teflon spacer, and placed in a copper sample cell holder. FT-IR spectra of all resulting solutions were collected at room temperature with a resolution of 0.24 cm^{-1}. All spectra were background subtracted by using the absorption spectrum of the solvent.

IIB. Polarization-Selective Pump−Probe (PSPP) Spectroscopy. A detailed description of the instrumental setup has been provided previously.[48,49] Briefly, a Ti:Sapphire oscillator/regenerative amplifier was used to produce pulses of 800 nm light with 2 mJ of energy and 3 kHz repetition rate. The output from the regenerative amplifier was converted from 800 nm to 4.6 μm (30 μJ and 3 kHz repetition rate) by using a home-built optical parametric amplifier (OPA). The mid-IR OPA output was tuned to 2155 cm^{-1}. It has a bandwidth of 100 cm^{-1}, and it is near transform limited.

The population decay of each probe was measured by using a polarization-selective pump−probe (PSPP) ultrafast IR experiment. The OPA output is split into a strong pump beam (∼90% intensity) and a weak probe beam (∼5% intensity). The pump beam is directed through a germanium acousto-optic modulator (AOM) for pulse shaping, which functions by blocking the resonant frequencies of every other pulse.[50] The probe is directed to a variable mechanical delay stage (range = ∼2 ns). Before the sample, the polarization of the pump pulse is rotated +45° relative to the probe pulse. A computer-controlled polarizer resolves the probe polarization after the sample at +45° (parallel) and −45° (perpendicular). The signal intensities, parallel ($I_{\parallel}(t)$) and perpendicular ($I_{\perp}(t)$), are measured.[3,4] The probe pulse is frequency resolved by using a monochromator and a 32-pixel mercury cadmium telluride (MCT) array detector. The time evolution of the parallel and perpendicular pump−probe signals is obtained by increasing the time delay, t, between pump and probe pulses by using the mechanical delay stage mentioned above. The population decay, $P(t)$ (lifetime), is given by

$$P(t) = \frac{1}{3}(I_{\parallel} + 2I_{\perp}) \quad (1)$$

III. RESULTS AND DISCUSSION

IIIA. Vibrational Spectra. The infrared absorption spectra of all new selenocyanate probes in DMF are shown in Figure 2, with fits using a Voigt function. The fit parameters are

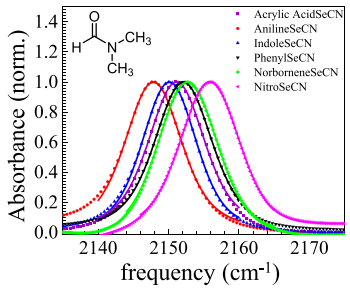

Figure 2. Normalized linear absorption spectrum of the nitrile stretch of selenocyanate probes in DMF. The spectra are well-described by a Voigt function. The fitting parameters are shown in Table 1.

presented in Table 1. The spectra for the probes in DMSO are quite similar. Parameters for the probes in DMSO are also given in Table 1. All probes display a single vibrational resonance from the stretching mode of the CN moiety in the vicinity of 2150 cm^{-1}, which is consistent with the vibrational frequency of PhenylSeCN in non-hydrogen-bonding solvents.[51,52] In DMF, the PhenylSeCN spectrum is centered at 2152 cm^{-1}. AnilineSeCN displays the lowest vibrational frequency at 2148 cm^{-1}, followed by IndoleSeCN and Acrylic AcidSeCN, which are centered at 2150 and 2151 cm^{-1}, respectively. NorborneneSeCN and NitroSeCN shift to higher frequency relative to PhenylSeCN, with absorption maxima at 2153 and 2156 cm^{-1}, respectively. The full width at half-maxima (FWHM) of all probes are similar to that of PhenylSeCN, ∼9.5 cm^{-1},[51,52] and range from 9.1 to 10.0 cm^{-1} in DMF (see Table 1).

The spectral shifts can be rationalized in terms of Hammett parameters. Historically, the Hammett equation has been used to investigate the electronic effects on reaction rates at the *meta* and *para* positions of substituted benzene systems[53] and is typically written as

https://doi.org/10.1021/acs.jpcb.1c04939
J. Phys. Chem. B 2021, 125, 8907−8918

Table 1. Spectroscopic Properties of Selenocyanate Vibrational Probes in Several Solvents

probe	solvent	ω (cm^{-1})	FWHM (cm^{-1})	τ_1 (ps)	$\lvert\mu_{01}\rvert^2$ ($\times 10^{-3}$ D^2)	ε (M^{-1} cm^{-1})
PhenylSeCN	DMF	2152 ± 0.1	9.8 ± 0.03	377 ± 1	3.4 ± 0.2	51.5 ± 0.2
	DMSO	2150 ± 0.1	11.3 ± 0.05	420 ± 1		
	CCl_4	2151 ± 0.1	7.3 ± 1.20	734 ± 1		
	$CHCl_3$	2158 ± 0.1	9.5 ± 0.13	661 ± 1		
AnilineSeCN	DMF	2148 ± 0.1	9.6 ± 0.03	457 ± 1	3.7 ± 0.3	55.8 ± 0.2
	DMSO	2146 ± 0.1	9.6 ± 0.04	469 ± 1		
	CCl_4	2156 ± 0.1	7.0 ± 0.2	1235 ± 1		
	$CHCl_3$	2153 ± 0.1	10.5 ± 0.05	908 ± 1		
IndoleSeCN	DMF	2150 ± 0.1	9.1 ± 0.03	456 ± 1	3.4 ± 0.3	43.6 ± 0.2
	DMSO	2148 ± 0.1	10.8 ± 0.02	506 ± 1		
Acrylic AcidSeCN	DMF	2151 ± 0.1	9.5 ± 0.03	388 ± 1	3.9 ± 0.3	48.5 ± 0.2
	DMSO	2149 ± 0.1	11.1 ± 0.08	422 ± 1		
NorborneneSeCN	DMF	2153 ± 0.1	9.8 ± 0.02	414 ± 2	3.7 ± 1.0	43.4 ± 0.2
	DMSO	2150 ± 0.1	11.1 ± 0.18	462 ± 1		
NitroSeCN	DMF	2156 ± 0.1	10.0 ± 0.01	367 ± 1	2.9 ± 0.7	30.5 ± 0.1
	DMSO	2154 ± 0.1	11.5 ± 0.07	430 ± 1		

$$\log k = \rho\sigma_R + \log k_0 \quad (2)$$

with k the rate constant of the reaction with different substituents R, k_0 the rate constant of an unsubstituted compound, and ρ the sensitivity constant, which in this study quantifies the susceptibility of the CN vibrational frequency and the ipso ^{13}C NMR chemical shift to the nature of the *p*-substituent. The application of Hammett constants to properties other than rates of reactions has been used successfully to investigate electronic substitution effects for ^1H NMR and vibrational frequencies for a number of compounds.[54−57] The *p*-substituted phenyl selenocyanates offer good solubility in a variety of solvents, which allows the correlation between the substituent and the Hammett constant to be observed in different chemical environments.

The IR center frequency shift of the CN stretching mode (ω) and the ^{13}C chemical shift of the ipso carbon (δ, ppm) in DMSO are plotted against the Hammett parameter, σ_p, for the nitro, aniline, acrylic acid, and norbornene selenocyanate probes in Figures 3A and 3B, respectively. We chose to use *p*-substituted PhenylSeCN analogues, as the σ_p constants represent the net influence of both inductive and resonance effects, while the σ_m constant is limited to the inductive effect of the substituent alone.[58] The IndoleSeCN probe does not fit the structural requirement of a *p*-substituted PhenylSeCN molecule, and it is not included in these plots. Hammett plots for the vibrational frequency in dimethylformamide, chloroform, and dichloromethane as well as a Hammett plot for the ^{13}C chemical shifts in $CHCl_3$ are presented in the Supporting Information. The results in all solvents show equally good correlations with identical slopes.

The vibrational frequency is determined by the CN bond order and can be understood in light of the NMR ipso carbon chemical shifts. The carbon chemical shift is governed by the electron density on the atom, which in this case determines the extent of cross-conjugation between the selenium atom and the phenyl ring. An upfield shift results from a larger electron density at the ipso carbon (from the *p*-substituent), and it indicates less cross-conjugation from the selenium atom into the phenyl ring. Consequently, the selenium lone pair electrons can, by resonance, participate in the CN bond, thus decreasing its triple-bond character and vibrational frequency. Therefore, a stronger electron-donating character of the *p*-substituent is expected to decrease cross-conjugation (upfield chemical shift) and red-shift the vibrational frequency, and vice versa. The Hammett correlation and the absorption spectra indicate that the vibrational frequency shift of a PhenylSeCN molecule is determined by the electron-donating and -withdrawing ability of the *p*-substituent. It is important to note that since hydrogen bonding is known to affect the vibrational frequency of nitriles,[23,38,42,59] these results are only valid for non-hydrogen-bonding solvents.

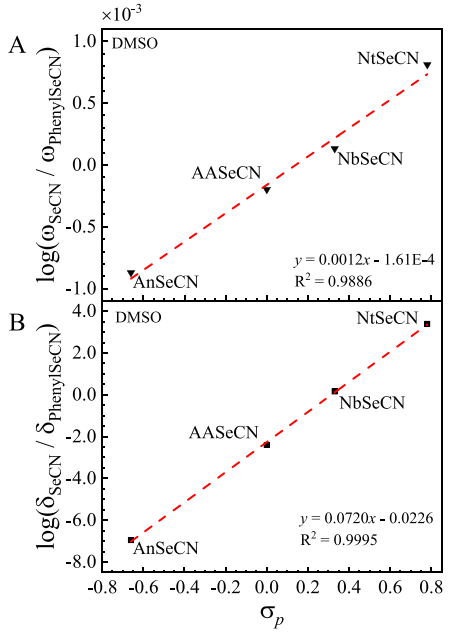

Figure 3. Hammett correlation of the σ_p constant with (A) vibrational frequency of the CN stretch and (B) ipso carbon ^{13}C chemical shift in DMSO. Hammett constants for σ_p were taken from the literature.[57] Both the vibrational frequency and the ^{13}C chemical shift displayed excellent correlation with σ_p. For clarity, the names of the probes have been further abbreviated. An: aniline; AA: acrylic acid; Nb: norbornene; Nt: nitro.

IIIB. Vibrational Lifetimes. The vibrational lifetime decay, τ_1, of each probe in DMF was measured by using PSPP spectroscopy (eq 1), and the results are shown in Figure 4. The lifetimes in DMF and DMSO are given in Table 1. The plot shows the normalized population decay dynamics of the

https://doi.org/10.1021/acs.jpcb.1c04939
J. Phys. Chem. B 2021, 125, 8907−8918

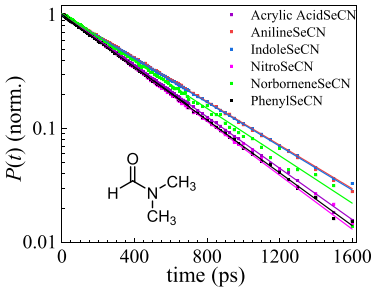

Figure 4. First vibrational excited state population decay of selenocyanate probes' CN stretch in DMF. The decays are single exponentials. Fits to the decays give the vibrational lifetimes. The lifetimes in DMF and DMSO are given in Table 1.

center frequency of the 1−2 vibrational transition. The 1−2 transition has the same lifetime as the 0−1 transition as both decays result from population decay from the 1 level to the 0 level. The 1−2 transition was used because it is less susceptible to solvent heating effects. An isotropic heating signal that results from background solvent absorption was observed in the PSPP experiment, which manifests as an early time deviation from exponential decay and a long-time constant offset.[5] Using a combination of a recently developed pulse-shaping method and data processing,[5,50] we removed the background heating signal to obtain the population decays presented in Figure 4 and given in Table 1.

The resulting population dynamics are a single-exponential decay. In DMF, the lifetime of PhenylSeCN is 377 ± 1 ps. Acrylic AcidSeCN and NorborneneSeCN have lifetimes of 388 ± 1 and 414 ± 2 ps, respectively, while IndoleSeCN and AnilineSeCN displayed somewhat longer lifetimes of 456 ± 1 and 457 ± 1 ps, respectively. NitroSeCN has the shortest lifetime in DMF with 367 ± 1 ps.

While we were able to increase the lifetime of the nitrile stretch vibration by changing the structure of the molecule, a systematic understanding of the relation between chemical structure and vibrational lifetime was not possible. The Hammett parameters were only mildly correlated to the vibrational lifetime in both DMF and DMSO, as shown in Figure 5. The results of the Hammett plots in Figure 3 show that in a particular solvent the vibrational frequency and the chemical shift are dominated by the structure of the molecules

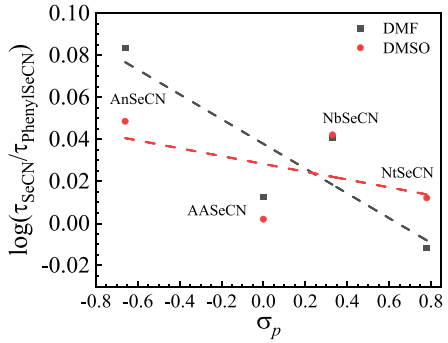

Figure 5. Hammett correlation of the σ_p constant with the lifetime of the first excited state of the selenocyanate probes' CN stretch in DMF and DMSO. For clarity, the names of the probes have been further abbreviated. An: aniline; Nb: norbornene; Nt: nitro; AA: acrylic acid. It can be seen that the CN vibrational lifetime is not well correlated to σ_p.

alone. However, vibrational relaxation depends on the coupling of the relaxing mode, CN, to both intra- and intermolecular modes, which is why Figure 5 shows that the vibrational lifetime is only weakly correlated to σ_p, as this parameter cannot capture the interactions between the probe and the solvent. Vibrational relaxation requires the energy of initially excited modes to be conserved by a combination of creation and annihilation of other modes.[37] These modes are vibrations of the molecule containing the excited mode and low-frequency modes of the solvent continuum, and possibly molecular vibrations of solvent molecules.[37,44] There are three key factors in the rate of relaxation of an excited vibration: the anharmonic coupling strengths of the excited mode to inter- and intramolecular modes, the number of modes required to conserve energy (order of the process), and the density of states of the continuum modes. Having more modes required in the relaxation process, a weaker coupling between the excited mode and accepting modes and a low density of states result in longer lifetimes.[37]

To our knowledge, no other vibrational probes display such long lifetimes as the new selenocyanate structures under room temperature conditions in complex solvents. These long vibrational lifetimes are attributed to the well-known effect of a heavy atom, which in this case is the selenium atom.[16] Kossowska et al. observed a 2-fold increase in the vibrational lifetime of a phenyl alkyne molecule by introducing a sulfur atom, and a 17-fold increase by introduction of a selenium atom between the alkyne and the phenyl ring. Still, the longest lifetime achieved was 94.2 ps.[16,24,25] Chalyavi et al. employed the introduction of heavy atoms to extend the lifetime of azides and observed that when a carbon atom is replaced by Sn in a triphenyl azide molecule, there was a 2-fold increase in the vibrational lifetime from 2 to 4 ps.[27] For comparison, benzonitrile (BZN) was previously reported to have a 5.6 ps lifetime in a non-hydrogen-bonding system,[36] which is consistent with the lifetime of other nitriles.[16,52,60] Compared to BZN, incorporation of a selenium atom to make PhenylSeCN causes a ∼67-fold increase in the vibrational lifetime to 377 ± 1 ps (Table 1). Incorporation of a heavy atom isolates the CN stretch. The effect is caused by decoupling the CN stretch from the high density of accepting modes of the rest of the molecule, retarding intramolecular vibrational relaxation pathways.[25,37] Comparison to the studies mentioned above suggests that the heavy-atom effect has a larger impact on phenyl nitriles than on phenyl alkynes and azides. A discussion of the possible reasons for the long lifetimes of the new -SeCN probes is provided below.

To motivate this discussion, it is interesting to first compare the vibrational relaxation of $W(CO)_6$ in simple and complex solvents to the relaxation of two of the -SeCN probes: PhenylSeCN, which is commercially available, and AnilineSeCN, which is the *p*-substituted probe with the longest lifetime of the probes in both DMF (457 ps) and DMSO (469 ps). $W(CO)_6$ has a room-temperature lifetime of 700 ps in CCl_4. Prior to this work, to our knowledge, 700 ps was the longest vibrational lifetime for a molecule in a room-temperature liquid. PhenylSeCN in room-temperature CCl_4 displayed a CN stretch lifetime of 734 ps, just slightly longer than that of $W(CO)_6$. Notably, the AnilineSeCN lifetime in room-temperature CCl_4 is a remarkable 1235 ps. Again, to our knowledge, this is by far the longest vibrational lifetime measured in a room-temperature liquid.

https://doi.org/10.1021/acs.jpcb.1c04939
J. Phys. Chem. B 2021, 125, 8907−8918

CCl_4 is a very simple solvent, so it is important to consider how vibrational lifetimes change as the solvent becomes more complex. In $CHCl_3$, the $W(CO)_6$ lifetime decreases from 700 to 370 ps, which is a 47% decrease caused by a relatively small change in the nature of the solvent. In contrast, the PhenylSeCN lifetime decreases from 734 to 662 ps (10% decrease), and the AnilineSeCN lifetime decreases from 1235 to 908 ps (26% decrease).

Of more importance is what these molecules' lifetimes are in complex solvents, where there are more notable differences. PhenylSeCN has lifetimes of 377 and 420 ps in DMF and DMSO, respectively. The lifetimes of $W(CO)_6$ in these solvents have not been measured. However, for similarly complex solvents, the $W(CO)_6$ lifetimes are much shorter, with 150 ps in 2-methylpentane,[61] 110 ps in the alkane region of a dilauroylphosphatidylcholine bilayer,[62] and 85 ps in 2-methyltetrahydrofuran.[61]

What is really interesting about the selenocyanate probes is that while $W(CO)_6$ and PhenylSeCN have similar lifetimes in CCl_4, $W(CO)_6$'s lifetime is ~100 ps in complex solvents (85% decrease), whereas PhenylSeCN's lifetime remains at ~400 ps (45% decrease). $W(CO)_6$ and other metal carbonyls, which have even shorter lifetimes, have very large transition dipoles, while the -SeCN probes have moderately small transition dipoles (see section IIIC). However, in applications where the lifetime is the most important property of a vibrational probe, the -SeCN probes provide experimental windows that extend well past 1 ns. In addition, the CN of the -SeCN probes is a single local mode, whereas the metal carbonyls generally have three or more IR-active modes because they contain three or more CO moieties. $W(CO)_6$ has only one IR-active mode, but it is triply degenerate, which causes a number of complications. Additionally, $W(CO)_6$ has Raman-active modes 32 and 136 cm^{-1} higher in energy than the IR-active mode asymmetric stretch at 1935 cm^{-1}, which enables rapid transfer of the initial IR excitation of the asymmetric stretch to one of the Raman-active modes.[35]

To give a feel for the considerations involved in the changes in the vibrational lifetime going from simple to complex solvents, a heuristic discussion of PhenylSeCN will be given, as the necessary low-frequency modes that are directly coupled to the CN stretch are known.[63] There are three relevant vibrational modes: the Se-CN stretch frequency at 523 cm^{-1}, the Se−C−N in-plane bend at 390 cm^{-1}, and the Se−C−N out-of-plane bend at 349 cm^{-1}. To conserve energy, the CN stretch is annihilated, and enough intra- and intermolecular modes must be created and annihilated to equal the frequency of the CN stretch. Modes of the phenyl ring will not be considered, as they will only be indirectly and very weakly coupled to the CN via motions of the Se. As several quanta of the modes given above can be excited, it is necessary to reduce the frequency of higher quantum number modes by the anharmonicities. As the anharmonicities are not know, it is assumed that they are the same percentage of the frequency as the anharmonicity of the CN stretch, 1.2%, which is known from nonlinear experiments (see the Supporting Information). In addition, the theoretically calculated density of states of the continua of modes for CCl_4 and $CHCl_3$ will be used.[44] The density of states of both liquids rise steeply from zero frequency to broad maxima at ~30 cm^{-1} and then have long tails to high frequency. The CCl_4 density of states goes to zero at ~130 cm^{-1}, and the $CHCl_3$ density of states goes to zero at ~180 cm^{-1}.

First consider the relaxation pathway of PhenylSeCN in CCl_4 (υ_{CN} = 2151 cm^{-1}) in which the CN stretch is annihilated and four quanta of the Se−CN stretch are created. Taking the Se−CN stretch anharmonicity to be 6 cm^{-1}, the total energy in the four quanta is 2074 cm^{-1}, leaving a deficit of 77 cm^{-1}. This energy is obtained by the creation of a mode of the continuum of 77 cm^{-1}, which is within the CCl_4 density of states. This is a sixth-order process, i.e., annihilation of the CN stretch, and creation of 4 Se-CN stretches and one mode of the continuum. When written out in detail, there are anharmonic coupling constants, one annihilation operator, and five creation operators.[37] The 77 cm^{-1} continuum mode is at ~40% of the peak of the density of states, a value of ~0.0017 in the units of ref 44. If this same mechanism occurred in $CHCl_3$ (υ_{CN} = 2158 cm^{-1}), an 84 cm^{-1} mode from the continuum would be required, which in the density of states also has a value of ~0.0017. This would suggest that the lifetime of PhenylSeCN would be about the same in both $CHCl_3$ and CCl_4. The experimental results show that the lifetime in $CHCl_3$ is 10% faster than in CCl_4. However, this mechanism assumes that the coupling to the continuum modes is the same in the two liquids. Because the natures of the modes of the continuum of the two liquids are different, it is unlikely the coupling constants will be the same. However, qualitatively, this example shows how the lifetime can change when going between two very similar liquids.

Let us consider two of the many other possible relaxation pathways for PhenylSeCN in CCl_4. The first is to create three Se−CN stretches and two Se−C−N out-of-plane bends, with an anharmonicity of 4 cm^{-1} for the latter. The combination of these modes gives a total energy of 2251 cm^{-1}. Therefore, a 100 cm^{-1} mode of the solvent continuum must be annihilated to conserve energy. At room temperature, k_BT is ~200 cm^{-1}, so a 100 cm^{-1} mode will be populated. This is a seventh-order process, i.e., five creations and two annihilations. In general, a lower-order process is more favorable. Additionally, the density of states at 100 cm^{-1} is very small, which makes it likely that the sixth-order process considered above would be preferred.

Another possibility is a sixth-order process where three Se−CN stretches plus a 635 cm^{-1} intramolecular mode of CCl_4 are created.[44,64] This would require annihilation of a 41 cm^{-1} mode of the continuum, which is near (~95%) the peak of the density of states. In $CHCl_3$, the intramolecular mode is found at 667 cm^{-1}, which requires a 66 cm^{-1} mode of the continuum to be annihilated. This mode is found at only ~73% of the density of states in $CHCl_3$. If the couplings are the same in both solvents, this pathway would make the relaxation in $CHCl_3$ slower than in CCl_4 rather than the experimentally observed 10% faster. Therefore, the coupling to the intramolecular mode in $CHCl_3$ would have to be substantially larger to make this pathway viable.

The pathways described above are only examples of the many possible pathways that could participate in the vibrational relaxation process. They are intended to illustrate the factors that come into play when considering changes in vibrational lifetimes going from one solvent to another. Now, we consider what happens when we compare different vibrational probes, and use AnilineSeCN for this comparison. First, we need to determine the relevant frequencies of the modes that are coupled to the CN stretching mode. The Hammett plot (Figure 3B) implies that the electron density on the Se is significantly different for PhenylSeCN and

https://doi.org/10.1021/acs.jpcb.1c04939
J. Phys. Chem. B 2021, 125, 8907−8918

AnilineSeCN in the solvents studied, and such a change is expected to be correlated to a shift in the three low-frequency modes of AnilineSeCN compared to PhenylSeCN.

To confirm this, the vibrational modes of PhenylSeCN and AnilineSeCN were obtained by using DFT calculations (see the Supporting Information). The calculations yielded a frequency of 534 and 520 cm^{-1} for the Se−CN stretch of PhenylSeCN and AnilineSeCN, respectively. In PhenylSeCN, the calculation is only 2.1% higher than the experimental value mentioned above. Additionally, like we did for PhenylSeCN, the anharmonicity of the Se−CN stretch mode in AnilineSeCN is assumed to be the same as in the CN stretch (1.2% from nonlinear experiments; see the Supporting Information). Therefore, assuming the same percent error in the DFT calculation for both probe molecules, we obtain a Se−CN frequency of 509 cm^{-1} with an anharmonicity of 6 cm^{-1} for AnilineSeCN.

AnilineSeCN's lifetime decreases from 1235 to 908 ps in going from CCl_4 to $CHCl_3$, a much larger percentage change than seen for PhenylSeCN. In the first relaxation mechanism discussed above, four Se−CN stretches and a 77 cm^{-1} mode of the continuum are created to conserve energy in the CN relaxation of PhenylSeCN in CCl_4. In this case, the continuum mode was in the tail of the density of states distribution. Considering the same first relaxation mechanism for the CN vibration in CCl_4 (υ_{CN} = 2156 cm^{-1}) of AnilineSeCN as for PhenylSeCN, the annihilation of four Se−CN stretches provides 2018 cm^{-1}, leaving a deficit of 138 cm^{-1}. However, the density of states in CCl_4 vanishes at 130 cm^{-1}. Therefore, the relaxation of AnilineSeCN's CN stretch in CCl_4, via this mechanism, would likely require two modes of the solvent continuum to conserve energy. This path would be seventh order, which, as observed, would make the CN lifetime much longer in AnilineSeCN than in PhenylSeCN. By contrast, in $CHCl_3$ (υ_{CN} = 2153 cm^{-1}), a 135 cm^{-1} mode would be required, which is within the available density of states (the density of states vanishes at 180 cm^{-1}). In this case, only one mode of the continuum would be required, and the process would become sixth order, likely resulting in a significantly faster lifetime decay of AnilineSeCN in $CHCl_3$ than in CCl_4, as observed. Again, there are many pathways that could participate in the vibrational relaxation mechanism of these probes, and this discussion is intended to highlight the type of changes that can occur when the *p*-substituent in PhenylSeCN changes.

It is possible that the reason for the -SeCN probes to have such long lifetimes is that they have only three intramolecular modes directly coupled to the CN stretch, all of which are below ~500 cm^{-1} and therefore result in high-order relaxation processes. In contrast, $W(CO)_6$ has 27 modes below ~500 cm^{-1}, which are directly coupled to the high-frequency triply degenerate CO asymmetric stretch.[44,64] These modes are distributed over a wide range of frequencies such that if in going from CCl_4 to $CHCl_3$ some of the 27 coupled modes can combine with the 1215 cm^{-1} C−H bend, then the order of the process could be reduced to fifth or even fourth order, greatly speeding up the vibrational relaxation. This could explain why $W(CO)_6$ has a very large lifetime change in going from CCl_4 to $CHCl_3$, whereas the small number of low-frequency modes in the -SeCN molecules that are directly coupled to the CN stretch makes such low-order relaxation pathways unlikely. If the intramolecular high-frequency phenyl ring modes of the -SeCN probes were coupled to the CN stretch, the lifetime of these probes could be reduced greatly by lowering the order of the relaxation pathway (likely the reason benzonitrile has such a short lifetime). However, the long -SeCN lifetimes strongly suggest that no such coupling exists.

In complex solvents of mainly light atoms, the − SeCN probes have lifetimes in the range ~400 to 500 ps. In these solvents, the continuum of intermolecular modes will extend to higher frequency than in CCl_4 and $CHCl_3$, and there will be more intramolecular solvent modes. These two factors would be expected to speed up the CN stretch population decay. However, there are still only 3 modes of the − SeCN probes that are directly coupled to the CN stretch. This fact suggests that even in more complex solvents, it is less likely to have a very low order relaxation pathway with strong couplings to produce a short lifetime. Therefore, it may be the small number of intramolecular modes directly coupled to the CN stretch that is responsible for the long lifetimes of the − SeCN probes in complex liquids.

IIIC. Transition Dipole Strength Calculation. The transition dipole strength of each probe was determined relative to the transition dipole strength of phenyl selenocyanate. The linear FT-IR, $\chi^{(1)}$, and nonlinear PSPP, $\chi^{(3)}$, signal amplitudes are proportional to the molecular transition dipole, $|\mu_{01}|$, by the following expressions:

$$\chi^{(3)} \propto |\mu_{01}|^4 \times C \times l$$
$$\chi^{(1)} \propto |\mu_{01}|^2 \times C \times l \tag{3}$$

where C is the concentration of the probe and l is the path length. Dividing $\chi^{(3)}$ by $\chi^{(1)}$, we obtain a signal amplitude equal to $|\mu_{01}|^2$ for each probe, and all constants are eliminated. All pump−probe signal amplitudes were obtained with identical laser conditions to avoid introducing distortions in the calculation due to changes in laser alignment or power. Normalizing all values to PhenylSeCN, we obtain the square of the transition dipole strength of each probe relative to that of PhenylSeCN. The transition dipole strength of PhenylSeCN was determined independently from its absorption spectrum in a sample of known concentration according to the following expressions:[65,66]

$$|\mu_{01}|^2 = 0.00917 \frac{D^2 \times \text{mol} \times \text{cm}}{L} \int \frac{\varepsilon(\nu)}{\nu} \, d\nu \tag{4}$$

$$\varepsilon(\nu) = \frac{A}{C \times l} \tag{5}$$

where A is the absorption of the probe, C is the concentration in units of mol/L, and l is the path length in units of cm. A full description of these calculations is presented in the Supporting Information, and the results are presented in Table 1. Equation 5 was also used to compute the molar extinction coefficient (ε) of all probes at the absorbance maximum frequency.

The disadvantage of the incorporation of a heavy atom in a nitrile molecule is that it results in a decrease of the molecule's transition dipole strength. This effect is not observed in alkynes and azides.[24,25] For comparison, we measured the transition dipole strength of BZN and obtained 0.0070 D^2. This value was in good agreement with a previous report of the transition dipole strength for BZN.[40] The transition dipole strength of PhenylSeCN was found to be ~2-fold smaller with

https://doi.org/10.1021/acs.jpcb.1c04939
J. Phys. Chem. B 2021, 125, 8907−8918

0.0034 D^2. Through resonance, the coupling of the CN moiety and the phenyl ring in BZN causes a decrease in the bond order of the nitrile, thus increasing its transition dipole strength.[59] On the other hand, the Se atom in PhenylSeCN interrupts this resonance by decoupling the CN from the phenyl ring, causing the nitrile to regain some triple-bond character, thus decreasing its transition dipole strength.[67]

Acrylic AcidSeCN and IndoleSeCN have a transition dipole strength of 0.0039 ± 0.0003 and 0.0034 ± 0.0003 D^2, respectively. Both AnilineSeCN and NorborneneSeCN have a transition dipole strength of 0.0037 ± 0.0003 D^2, and NitroSeCN displayed a value of 0.0029 ± 0.0007 D^2. The molar extinction coefficients of all probes were found in the range between ∼43 and ∼55 M^{-1} cm^{-1}, except for NitroSeCN with 30.5 M^{-1} cm^{-1}. While the transition dipole would be expected to also display a correlation with the Hammett parameters, the measured values were within error of each other, and no clear correlation was observed.

IIID. Stark Tuning Rate. The vibrational frequency of nitriles is sensitive to the electrostatics of their local environment, i.e., solvatochromism. In nitriles, this frequency shift is described by the first-order vibrational Stark effect, which has been shown to fully account for their solvatochromic behavior.[40] Analysis is performed by using the Onsager reaction field model, which considers the probe to be in a spherical cavity in the dielectric medium (i.e., the solvent). Quantification of the local environment sensitivity is achieved by calibrating the vibrational frequency of each probe in a series of solvents with varying static dielectric constant.[8,40]

Each probe was dissolved in a series of nonaromatic, non-hydrogen-bonding solvents, and their FT-IR spectra were collected. All spectra were background subtracted and fitted with a Voigt function. Following the method outlined by Levinson,[42] the electric field projected by the solvent onto the molecule is given by

$$\vec{F} = \frac{\vec{\mu}_0}{4\pi\varepsilon_0 a^3}\left[\frac{2(\varepsilon - 1)(n^2 + 2)}{3(2\varepsilon + n^2)}\right] \quad (6)$$

where $\vec{\mu}_0$ is the permanent dipole moment of the probe molecule, ε_0 is the permittivity of free space, a^3 is the Onsager cavity, which is related to the probe's size and density, ε is the static dielectric constant of the solvent, and n is the refractive index of the probe. The probes' absorption maxima were plotted as a function of their Onsager factor (square brackets term in eq 6). The slope of a linear fit to the data quantifies the sensitivity of the vibrational transition to the dielectric constant of the solvent.

The linear absorption spectra of the selenocyanate vibrational probes in solvents of different dielectric constants are presented in Figure 6. Nonaromatic and non-hydrogen-bonding solvents were used to avoid inducing probe−solvent interactions that influence the nitrile's vibrational frequency in ways that are not accounted for by the Stark effect. All probes were sensitive to the electrostatic characteristics of the solvent, and the vibrational transitions were shifted to higher frequencies with decreasing solvent polarity. The absorption spectra in the high-polarity regime were symmetric, while those of more nonpolar solvents displayed asymmetry, showing broadening of the low-frequency region of their absorption spectra. These behaviors are consistent with previously observed solvent-dependent vibrational shifts of

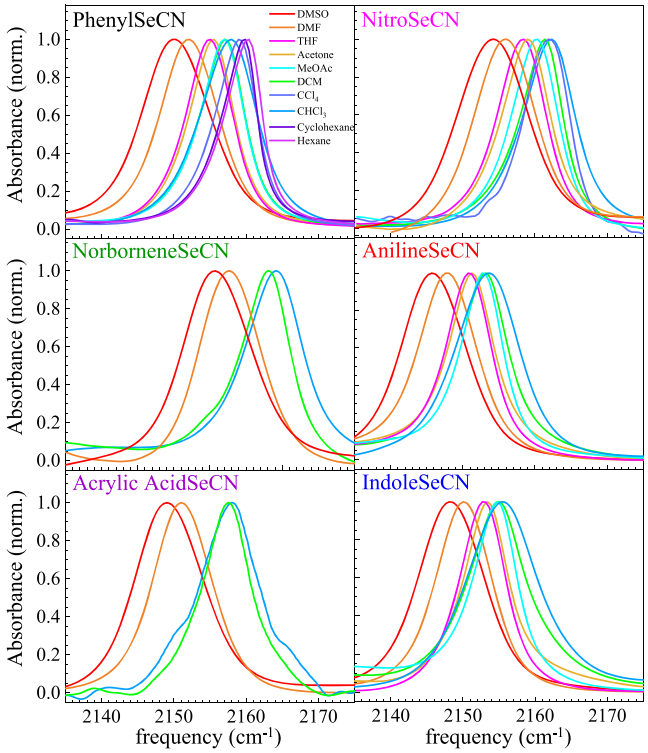

Figure 6. Normalized linear absorption spectra of symmetric stretch of nitrile moiety of selenocyanate probes in a series of non-hydrogen-bonding liquid solvents. The vibrational frequency maximum shifts from low to high frequency with decreasing solvent polarity. The vibrational frequency shifts are determined by the first-order Stark effect of nitriles.

nitriles.[40] The parametrization of all absorption spectra is provided in the Supporting Information.

A plot of the Onsager factor (square brackets term in eq 6) against the center frequency is shown in Figure 7. The

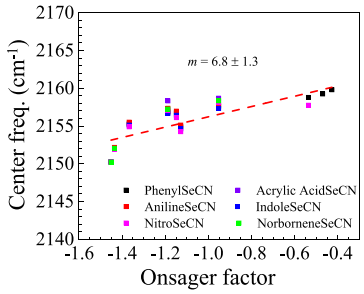

Figure 7. Vibrational transition frequencies of the nitrile stretch of selenocyanate probes as a function of Onsager factor (square brackets term in eq 6). The data for all new selenocyanate structures were vertically shifted to match that of phenyl selenocyanate at the lowest Onsager factor to better highlight the similarity in sensitivity to electrostatic environment among structures.

solubility of the new probes was poor in carbon tetrachloride, cyclohexane, and hexane. Acrylic AcidSeCN and NorborneneSeCN were insoluble in most of the solvents used, and their absorption spectra were only obtained in DMSO, DMF, DCM, and $CHCl_3$.

A comparison of the solvatochromic sensitivity (slope) of the new selenocyanate probes to that of PhenylSeCN was possible by shifting the data for each new probe by a vertical

https://doi.org/10.1021/acs.jpcb.1c04939
J. Phys. Chem. B 2021, 125, 8907−8918

offset to make its frequency at the lowest Onsager factor value coincident with the PhenylSeCN frequency. A plot of the original data is provided in the Supporting Information. It can be seen that all absorption maxima for each probe trace the behavior of PhenylSeCN as a function of the Onsager factor reasonably well. Following the procedure outlined by Levinson et al., a linear fit was performed on the PhenylSeCN data to quantify its sensitivity to local electrostatics.[40] The slope of the Onsager plot for PhenylSeCN is 7.21 ± 1.38. For comparison, Levinson reported an Onsager plot slope of 4.9 for BZN using the same solvent systems.[40] It was not possible to calculate the Stark tuning rate of the new vibrational probes, as this property depends on additional and currently unavailable information, such as the probe's density and permanent dipole moment (see eq 6). Previously, however, the Stark tuning rate of PhenylSeCN was found to be 12.3 ± 2.4 $cm^{-1}/(GV/m)$.[26] BZN has a Stark tuning rate of 5.7 $cm^{-1}/(GV/m)$, while typical values for Stark tuning rates of nitriles range between 4 and 7 $cm^{-1}/(GV/m)$.[40] It can be seen that the presence of the selenium atom causes an increase in the sensitivity to local environment electrostatics compared to other nitrile vibrational probes. Our results (Figure 7) show that the nitrile stretch vibrations of the new selenocyanate probes have identical sensitivity to local electrostatics as PhenylSeCN and should be expected to have similarly large Stark tuning rates.

IV. SYNTHESIS OF THE VIBRATIONAL PROBES

The five new probe molecules were synthesized by using modifications of methods that are available in the literature.[45,46,68] Here, only the schemes of the synthesis for each probe are presented (Schemes 1−5). Complete details of the synthesis of each probe are given in the Supporting Information. The synthetic procedures contain all necessary information to allow synthesis of the desired probe. In addition, complete ^{13}C and ^{1}H NMR characterizations, which confirm that the appropriate probe structure was produced by the synthetic procedure, are given in the Supporting Information.

Scheme 1. Synthesis of 3-Indole Selenocyanate

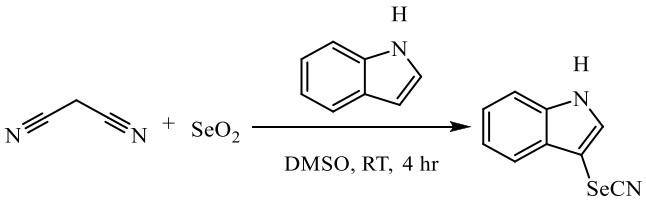

Scheme 2. Synthesis of *p*-Aniline Selenocyanate

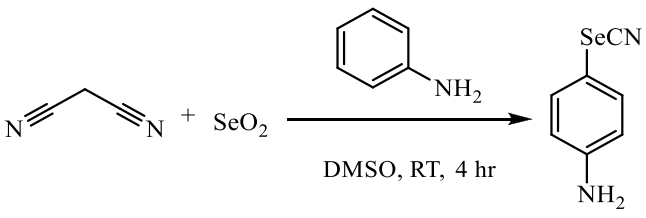

Scheme 3. Synthesis of (Z)-3-(4-Selenocyanatophenylcarbamoyl)acrylic Acid

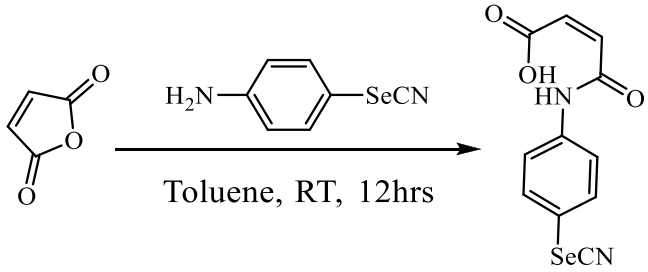

Scheme 4. Synthesis of Norbornene Dicarboximide−Phenyl Selenocyanate

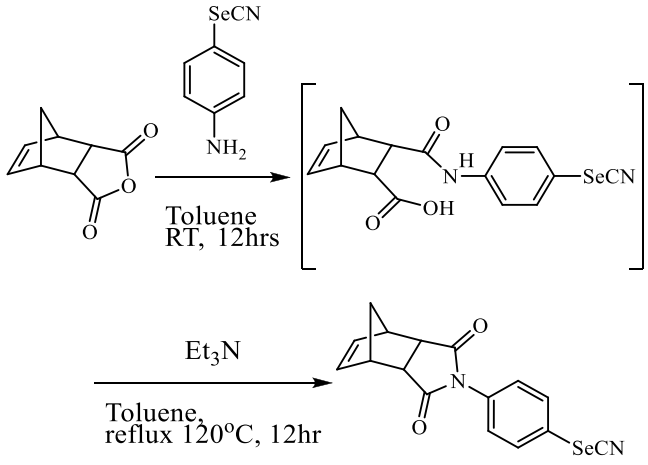

Scheme 5. Synthesis of *p*-Nitrophenyl Selenocyanate

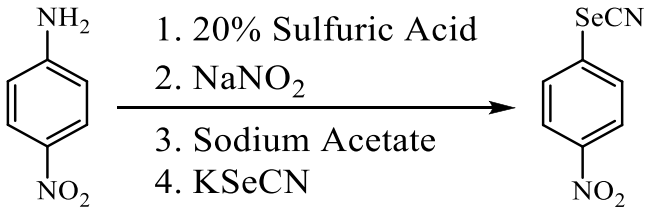

V. CONCLUSIONS

We presented the synthesis of five novel selenocyanate vibrational probe molecules and characterized their vibrational frequencies, excited state lifetimes, transition dipole strengths, and local environment sensitivities. The reporting moiety is the CN stretch. These novel structures were found to have long-lived vibrational first excited states in the range between 377 and 457 ps in DMF. To our knowledge, no previous vibrational probes have as long a lifetime at room temperature in complex solvents. In addition, one of the probes has a lifetime of 1235 ps in the simple solvent, CCl_4, which is the longest vibrational lifetime reported in a room temperature liquid. The long vibrational lifetimes result from the incorporation of a selenium atom between the nitrile and the rest of the structure, which is known to cause retardation of vibrational relaxation. Comparison to previously measured lifetimes of benzonitrile in other non-hydrogen-bonding systems indicates that selenium increases the vibrational lifetime by ∼67-fold. A heuristic discussion is provided to explain the reasons for the long lifetimes in these -SeCN probes. Incorporation of the selenium atom also causes ∼2-

https://doi.org/10.1021/acs.jpcb.1c04939
J. Phys. Chem. B 2021, 125, 8907−8918

fold decrease of the transition dipole strength to an average of 3.6×10^{-3} D^2. Because the commercially available probe, PhenylSeCN, has successfully been used in the past to study vibrational dynamics by using IR nonlinear experiments,[5,69] we conclude that this decrease in transition dipole strength is not experimentally prohibitive.

The local environment sensitivity of the probes results from solvatochromic vibrational frequency shifts caused by the electrostatics of their immediate environment. All new structures were observed to have identical solvatochromic behavior as PhenylSeCN. It was not possible to calculate a Stark tuning rate, but our results suggest that all new probes should have an STR comparable to that of PhenylSeCN (12.3 ± 2.4 $cm^{-1}/(GV/m)$). This STR represents an ∼2-fold increase in local environment sensitivity compared to other nitrile vibrational probes.

Long-lived vibrational probes are essential for the study of structurally complex chemical systems with slow molecular dynamics, such as polymers and biological model membranes. The probes were observed to be essentially insoluble in water. For systems such as vesicles, they would be useful for studying the interiors of their organic leaflets[31] and how interior dynamics and interactions are influenced by e.g., the addition of transmembrane proteins.

These probes provide a significant increase in the vibrational lifetime and sensitivity to local electrostatics. Because the solvatochromic behavior and dipole strengths were indistinguishable among the new -SeCN probes, their relative usefulness for a specific application should be judged based on the chemical structure and vibrational lifetime. Some of the probes can be chemically bound to other species, which will enhance their utility.

■ ASSOCIATED CONTENT

Supporting Information

The Supporting Information is available free of charge at https://pubs.acs.org/doi/10.1021/acs.jpcb.1c04939.

> Synthetic procedures and nuclear magnetic resonance (NRM) spectra of all new selenocyanate probes, Hammett correlations of vibrational frequency and ipso ^{13}C chemical shift in additional solvents, vibrational anharmonicity, DFT calculations, transition dipole strength calculations, and solvatochromism (PDF)

■ AUTHOR INFORMATION

Corresponding Authors

Michael D. Fayer − *Department of Chemistry, Stanford University, Stanford, California 94305, United States;* orcid.org/0000-0002-0021-1815; Phone: 650 723-4446; Email: fayer@stanford.edu

Gregory Sotzing − *Department of Chemistry, University of Connecticut, Storrs, Connecticut 06269, United States;* Phone: 860 486-4619; Email: g.sotzing@uconn.edu

Authors

Sebastian M. Fica-Contreras − *Department of Chemistry, Stanford University, Stanford, California 94305, United States;* orcid.org/0000-0003-4177-8436

Robert Daniels − *Department of Chemistry, University of Connecticut, Storrs, Connecticut 06269, United States;* orcid.org/0000-0003-1114-5515

Omer Yassin − *Department of Chemistry, University of Connecticut, Storrs, Connecticut 06269, United States*

David J. Hoffman − *Department of Chemistry, Stanford University, Stanford, California 94305, United States;* orcid.org/0000-0001-8518-7676

Junkun Pan − *Department of Chemistry, Stanford University, Stanford, California 94305, United States*

Complete contact information is available at: https://pubs.acs.org/10.1021/acs.jpcb.1c04939

Author Contributions

S.M.F.-C. and R.D. have contributed equally to this work.

Notes

The authors declare no competing financial interest.

Data Availability. All relevant data are included in the paper and the SI Appendix. Infrared characterization data are available by contacting Professor Michael D. Fayer, Department of Chemistry, Stanford University, Stanford, CA 94305-5080; email fayer@stanford.edu. Organic synthesis data are available by contacting Professor Gregory Sotzing, Department of Chemistry, University of Connecticut, Storrs, CT 06269; email g.sotzing@uconn.edu.

■ ACKNOWLEDGMENTS

This work was supported by the Office of Naval Research by ONR: N00014-17-1-2656.

■ REFERENCES

(1) Adhikary, R.; Zimmermann, J.; Romesberg, F. E. Transparent Window Vibrational Probes for the Characterization of Proteins With High Structural and Temporal Resolution. *Chem. Rev.* **2017**, *117* (3), 1927−1969.

(2) Moilanen, D. E.; Fenn, E. E.; Lin, Y.-S.; Skinner, J. L.; Bagchi, B.; Fayer, M. D. Water Inertial Reorientation: Hydrogen Bond Strength and the Angular Potential. *Proc. Natl. Acad. Sci. U. S. A.* **2008**, *105* (14), 5295−5300.

(3) Tokmakoff, A. Orientational Correlation Functions and Polarization Selectivity for Nonlinear Spectroscopy of Isotropic Media. I. Third Order. *J. Chem. Phys.* **1996**, *105* (1), 1−12.

(4) Tan, H.-S.; Piletic, I. R.; Fayer, M. D. Polarization Selective Spectroscopy Experiments: Methodology and Pitfalls. *J. Opt. Soc. Am. B* **2005**, *22* (9), 2009−2017.

(5) Hoffman, D. J.; Fica-Contreras, S. M.; Fayer, M. D. Amorphous Polymer Dynamics and Free Volume Element Size Distributions From Ultrafast IR Spectroscopy. *Proc. Natl. Acad. Sci. U. S. A.* **2020**, *117* (25), 13949−13958.

(6) Baiz, C. R.; McRobbie, P. L.; Anna, J. M.; Geva, E.; Kubarych, K. J. Two-Dimensional Infrared Spectroscopy of Metal Carbonyls. *Acc. Chem. Res.* **2009**, *42* (9), 1395−1404.

(7) Maj, M.; Oh, Y.; Park, K.; Lee, J.; Kwak, K. W.; Cho, M. Vibrational Dynamics of Thiocyanate and Selenocyanate Bound to Horse Heart Myoglobin. *J. Chem. Phys.* **2014**, *140* (23), 235104.

(8) Williams, I. M.; Qasim, L. N.; Tran, L.; Scott, A.; Riley, K.; Dutta, S. C-D. Vibration at C2 Position of Imidazolium Cation as a Probe of the Ionic Liquid Microenvironment. *J. Phys. Chem. A* **2019**, *123* (29), 6342−6349.

(9) Kim, Y. S.; Hochstrasser, R. M. Applications of 2D IR Spectroscopy to Peptides, Proteins, and Hydrogen-Bond Dynamics. *J. Phys. Chem. B* **2009**, *113* (24), 8231−8251.

(10) Schmidt-Engler, J. M.; Zangl, R.; Guldan, P.; Morgner, N.; Bredenbeck, J. Exploring the 2D-IR Repertoire of the -SCN Label to Study Site-Resolved Dynamics and Solvation in the Calcium Sensor Protein Calmodulin. *Phys. Chem. Chem. Phys.* **2020**, *22* (10), 5463−5475.

(11) Blasiak, B.; Londergan, C. H.; Webb, L. J.; Cho, M. Vibrational Probes: From Small Molecule Solvatochromism Theory and Experiments to Applications in Complex Systems. *Acc. Chem. Res.* **2017**, *50* (4), 968−976.
(12) Chin, J. K.; Jimenez, R.; Romesberg, F. E. Direct Observation of Protein Vibrations by Selective Incorporation of Spectroscopically Observable Carbon−Deuterium Bonds in Cytochrome *c*. *J. Am. Chem. Soc.* **2001**, *123* (10), 2426−2427.
(13) Moilanen, D. E.; Wong, D.; Rosenfeld, D. E.; Fenn, E. E.; Fayer, M. D. Ion−Water Hydrogen-Bond Switching Observed With 2D IR Vibrational Echo Chemical Exchange Spectroscopy. *Proc. Natl. Acad. Sci. U. S. A.* **2009**, *106* (2), 375−380.
(14) Schmitz, A. J.; Hogle, D. G.; Gai, X. S.; Fenlon, E. E.; Brewer, S. H.; Tucker, M. J. 2D IR Study of Vibrational Coupling Between Azide and Nitrile Reporters in a RNA Nucleoside. *J. Phys. Chem. B* **2016**, *120* (35), 9387−9394.
(15) Fafarman, A. T.; Webb, L. J.; Chuang, J. I.; Boxer, S. G. Site-Specific Conversion of Cysteine Thiols into Thiocyanate Creates an IR Probe for Electric Fields in Proteins. *J. Am. Chem. Soc.* **2006**, *128* (41), 13356−13357.
(16) Ramos, S.; Scott, K. J.; Horness, R. E.; Le Sueur, A. L.; Thielges, M. C. Extended Timescale 2D IR Probes of Proteins: *p*-Cyanoselenophenylalanine. *Phys. Chem. Chem. Phys.* **2017**, *19* (15), 10081−10086.
(17) Knop, S.; Lindner, J.; Vöhringer, P. OH and NH Stretching Vibrational Relaxation of Liquid Ethanolamine. *Z. Phys. Chem.* **2011**, *225* (9−10), 913−926.
(18) Kooter, I. M.; Moguilevsky, N.; Bollen, A.; van der Veen, L. A.; Otto, C.; Dekker, H. L.; Wever, R. The Sulfonium Ion Linkage in Myeloperoxidase. Direct Spectroscopy Detection by Isotopic Labeling and Effect of Mutation. *J. Biol. Chem.* **1999**, *274* (38), 26794−26802.
(19) Lindquist, B. A.; Furse, K. E.; Corcelli, S. A. Nitrile Groups as Vibrational Probes of Biomolecular Structure and Dynamics: An Overview. *Phys. Chem. Chem. Phys.* **2009**, *11* (37), 8119−8132.
(20) Urbanek, D. C.; Vorobyev, D. Y.; Serrano, A. L.; Gai, F.; Hochstrasser, R. M. The Two Dimensional Vibrational Echo of a Nitrile Probe of the Villin HP35 Protein. *J. Phys. Chem. Lett.* **2010**, *1* (23), 3311−3315.
(21) Kearney, C.; Olenginski, L. T.; Hirn, T. D.; Fowler, G. D.; Tariq, D.; Brewer, S. H.; Phillips-Piro, C. M. Exploring Local Solvation Environments of a Heme Protein Using the Spectroscopic Reporter 4-Cyano-L-Phenylalanine. *RSC Adv.* **2018**, *8* (24), 13503−13512.
(22) Bazewicz, C. G.; Lipkin, J. S.; Smith, E. E.; Liskov, M. T.; Brewer, S. H. Expanding the Utility of 4-Cyano-L-Phenylalanine as a Vibrational Reporter of Protein Environments. *J. Phys. Chem. B* **2012**, *116* (35), 10824−10831.
(23) Lee, G.; Kossowska, D.; Lim, J.; Kim, S.; Han, H.; Kwak, K.; Cho, M. Cyanamide as an Infrared Reporter: Comparison of Vibrational Properties Between Nitriles Bonded to N and C Atoms. *J. Phys. Chem. B* **2018**, *122* (14), 4035−4044.
(24) Levin, D. E.; Schmitz, A. J.; Hines, S. M.; Hines, K. J.; Tucker, M. J.; Brewer, S. H.; Fenlon, E. E. Synthesis and Evaluation of the Sensitivity and Vibrational Lifetimes of Thiocyanate and Selenocyanate Infrared Reporters. *RSC Adv.* **2016**, *6* (43), 36231−36237.
(25) Kossowska, D.; Lee, G.; Han, H.; Kwak, K.; Cho, M. Simultaneous Enhancement of Transition Dipole Strength and Vibrational Lifetime of an Alkyne IR Probe via pi-d Backbonding and Vibrational Decoupling. *Phys. Chem. Chem. Phys.* **2019**, *21* (45), 24919−24925.
(26) Maj, M.; Ahn, C.; Blasiak, B.; Kwak, K.; Han, H.; Cho, M. Isonitrile as an Ultrasensitive Infrared Reporter of Hydrogen-Bonding Structure and Dynamics. *J. Phys. Chem. B* **2016**, *120* (39), 10167−10180.
(27) Chalyavi, F.; Schmitz, A. J.; Fetto, N. R.; Tucker, M. J.; Brewer, S. H.; Fenlon, E. E. Extending the Vibrational Lifetime of Azides With Heavy Atoms. *Phys. Chem. Chem. Phys.* **2020**, *22* (32), 18007−18013.
(28) Thon, R.; Chin, W.; Chamma, D.; Galaup, J. P.; Ouvrard, A.; Bourguignon, B.; Crepin, C. Vibrational Spectroscopy and Dynamics of $W(CO)_6$ in Solid Methane as a Probe of Lattice Properties. *J. Chem. Phys.* **2016**, *145* (21), 214306.
(29) Waegele, M. M.; Culik, R. M.; Gai, F. Site-Specific Spectroscopic Reporters of the Local Electric Field, Hydration, Structure, and Dynamics of Biomolecules. *J. Phys. Chem. Lett.* **2011**, *2* (20), 2598−2609.
(30) Park, K.-H.; Jeon, J.; Park, Y.; Lee, S.; Kwon, H.-J.; Joo, C.; Park, S.; Han, H.; Cho, M. Infrared Probes Based on Nitrile-Derivatized Prolines: Thermal Insulation Effect and Enhanced Dynamic Range. *J. Phys. Chem. Lett.* **2013**, *4* (13), 2105−2110.
(31) Kel, O.; Tamimi, A.; Fayer, M. D. Size-Dependent Ultrafast Structural Dynamics Inside Phospholipid Vesicle Bilayers Measured With 2D IR Vibrational Echoes. *Proc. Natl. Acad. Sci. U. S. A.* **2014**, *111* (3), 918−923.
(32) Abramczyk, H.; Paradowska-Moszkowska, K.; Wiosna, G. Premelting Structure: Vibrational Dynamics of Liquid, Undercooled Liquid, Glassy, and Crystal States in Methylcyclohexane and Deuterated Methylcyclohexane. *J. Chem. Phys.* **2003**, *118* (9), 4169−4175.
(33) Yamada, S. A.; Bailey, H. E.; Tamimi, A.; Li, C.; Fayer, M. D. Dynamics in a Room-Temperature Ionic Liquid From the Cation Perspective: 2D IR Vibrational Echo Spectroscopy. *J. Am. Chem. Soc.* **2017**, *139* (6), 2408−2420.
(34) Ando, R. A.; Brown-Xu, S. E.; Nguyen, L. N. Q.; Gustafson, T. L. Probing the Solvation Structure and Dynamics in Ionic Liquids by Time-Resolved Infrared Spectroscopy of 4-(Dimethylamino)-Benzonitrile. *Phys. Chem. Chem. Phys.* **2017**, *19* (36), 25151−25157.
(35) Tokmakoff, A.; Sauter, B.; Fayer, M. D. Temperature-Dependent Vibrational Relaxation in Polyatomic Liquids: Picosecond Infrared Pump−Probe Experiments. *J. Chem. Phys.* **1994**, *100* (12), 9035−9043.
(36) Sokolowsky, K. P.; Fayer, M. D. Dynamics in the Isotropic Phase of Nematogens Using 2D IR Vibrational Echo Measurements on Natural-Abundance ^{13}CN and Extended Lifetime Probes. *J. Phys. Chem. B* **2013**, *117* (48), 15060−15071.
(37) Kenkre, V. M.; Tokmakoff, A.; Fayer, M. D. Theory of Vibrational Relaxation of Polyatomic Molecules in Liquids. *J. Chem. Phys.* **1994**, *101* (12), 10618−10629.
(38) Bagchi, S.; Fried, S. D.; Boxer, S. G. A Solvatochromic Model Calibrates Nitriles' Vibrational Frequencies to Electrostatic Fields. *J. Am. Chem. Soc.* **2012**, *134* (25), 10373−10376.
(39) Getahun, Z.; Huang, C.-Y.; Wang, T.; De León, B.; DeGrado, W. F.; Gai, F. Using Nitrile-Derivatized Amino Acids as Infrared Probes of Local Environment. *J. Am. Chem. Soc.* **2003**, *125* (2), 405−411.
(40) Andrews, S. S.; Boxer, S. G. Vibrational Stark Effects of Nitriles I. Methods and Experimental Results. *J. Phys. Chem. A* **2000**, *104* (51), 11853−11863.
(41) Andrews, S. S.; Boxer, S. G. Vibrational Stark Effects of Nitriles II. Physical Origins of Stark Effects From Experiment to Perturbation Models. *J. Phys. Chem. A* **2002**, *106* (3), 469−477.
(42) Levinson, N. M.; Fried, S. D.; Boxer, S. G. Solvent-Induced Infrared Frequency Shifts in Aromatic Nitriles are Quantitatively Described by the Vibrational Stark Effect. *J. Phys. Chem. B* **2012**, *116* (35), 10470−10476.
(43) Gai, X. S.; Coutifaris, B. A.; Brewer, S. H.; Fenlon, E. E. A Direct Comparison of Azide and Nitrile Vibrational Probes. *Phys. Chem. Chem. Phys.* **2011**, *13* (13), 5926−5930.
(44) Moore, P.; Tokmakoff, A.; Keyes, T.; Fayer, M. D. The Low Frequency Density of States and Vibrational Population Dynamics of Polyatomic Molecules in Liquids. *J. Chem. Phys.* **1995**, *103* (9), 3325−3334.
(45) Kachanov, A. V.; Slabko, O. Y.; Baranova, O. V.; Shilova, E. V.; Kaminskii, V. A. Triselenium Dicyanide From Malononitrile and Selenium Dioxide. One-Pot Synthesis of Selenocyanates. *Tetrahedron Lett.* **2004**, *45* (23), 4461−4463.

https://doi.org/10.1021/acs.jpcb.1c04939
J. Phys. Chem. B 2021, 125, 8907−8918

(46) Schmid, G. H.; Garratt, D. G. Organoselenium Chemistry. 13. Reaction of Areneselenenyl Chlorides and Alkenes. An Example of Nucleophilic Displacement at Bivalent Selenium. *J. Org. Chem.* **1983**, *48* (23), 4169−4172.
(47) Kaushik, N. K.; Kaushik, N.; Attri, P.; Kumar, N.; Kim, C. H.; Verma, A. K.; Choi, E. H. Biomedical Importance of Indoles. *Molecules* **2013**, *18* (6), 6620−6662.
(48) Karthick Kumar, S. K.; Tamimi, A.; Fayer, M. D. Comparisons of 2D IR Measured Spectral Diffusion in Rotating Frames Using Pulse Shaping and in the Stationary Frame Using the Standard Method. *J. Chem. Phys.* **2012**, *137* (18), 184201.
(49) Yan, C.; Thomaz, J. E.; Wang, Y. L.; Nishida, J.; Yuan, R.; Breen, J. P.; Fayer, M. D. Ultrafast to Ultraslow Dynamics of a Langmuir Monolayer at the Air/Water Interface Observed With Reflection Enhanced 2D IR Spectroscopy. *J. Am. Chem. Soc.* **2017**, *139* (46), 16518−16527.
(50) Hoffman, D. J.; Fica-Contreras, S. M.; Pan, J.; Fayer, M. D. Pulse-Shaped Chopping: Eliminating and Characterizing Heat Effects in Ultrafast Infrared Spectroscopy. *J. Chem. Phys.* **2020**, *153* (20), 204201.
(51) Bian, H.; Wen, X.; Li, J.; Zheng, J. Mode-Specific Intermolecular Vibrational Energy Transfer. II. Deuterated Water and Potassium Selenocyanate Mixture. *J. Chem. Phys.* **2010**, *133* (3), No. 034505.
(52) Deàk, J. C.; Iwaki, L. K.; Dlott, D. D. Vibrational Energy Redistribution in Polyatomic Liquids: Ultrafast IR-Raman Spectroscopy of Acetonitrile. *J. Phys. Chem. A* **1998**, *102* (42), 8193−8201.
(53) Hammett, L. P. Some Relations Between Reaction Rates and Equilibrium Constants. *Chem. Rev.* **1935**, *17* (1), 125−136.
(54) Setliff, F. L.; Soman, N. G.; Caldwell, J. Z.; Rogers, D. L. Hammett Correlations in the ^{1}H NMR Spectra of Some N-Arlydihalonicotinamides. *JAAS* **1992**, *46* (11), 72−74.
(55) Huang, S.; Wong, J. C.; Leung, A. K.; Chan, Y. M.; Wong, L.; Fernendez, M. R.; Miller, A. K.; Wu, W. Excellent Correlation Between Substituent Constants and Pyridinium *N*-Methyl Chemical Shifts. *Tetrahedron Lett.* **2009**, *50* (35), 5018−5020.
(56) Dijk, T. v. Experimental and Theoretical Studies in Optical Coherence Theory. *Vrije Universiteit Amsterdam* **2011**, 15500−15524.
(57) Shawali, A. S.; Eweiss, N. F. Carbonyl Stretching Frequencies in Acyl- and Aryl-Substituted Phenyl Benzoates. *Can. J. Chem.* **1977**, *55*, 3967−3972.
(58) Hammett, L. P. The Effect of Structure Upon the Reactions of Organic Compounds. Benzene Derivatives. *J. Am. Chem. Soc.* **1937**, *59* (1), 96−103.
(59) Kryachko, E. S.; Nguyen, M. T. Hydrogen Bonding in Benzonitrile−Water Complexes. *J. Chem. Phys.* **2001**, *115* (2), 833−841.
(60) Lenchenkov, V.; She, C.; Lian, T. Vibrational Relaxation of CN Stretch of Pseudo-Halide Anions (OCN-, SCN-, and SeCN-) in Polar Solvents. *J. Phys. Chem. B* **2006**, *110* (40), 19990−19997.
(61) Tokmakoff, A.; Fayer, M. D. Homogenoeus Vibrational Dynamics and Inhomogeneous Broadening in Glass-Forming Liquids: Infrared Photon Echo Experiments From Room Temperature to 10K. *J. Chem. Phys.* **1995**, *103* (8), 2810−2826.
(62) Kel, O.; Tamimi, A.; Thielges, M. C.; Fayer, M. D. Ultrafast Structural Dynamics Inside Planar Phospholipid Multibilayer Model Cell Membranes Measured With 2D IR Spectroscopy. *J. Am. Chem. Soc.* **2013**, *135* (30), 11063−11074.
(63) Aynsley, E. E.; Greenwood, N. N.; Spragu, M. J. Reaction of Organomercury Compounds With Covalent Selenocyanates. *J. Chem. Soc.* **1965**, No. 0, 2395−2402.
(64) Smith, J. M.; Jones, L. H. Anharmonic Corrections for Fundamental Vibrations of the Metal Hexacarbonyls. *J. Mol. Spectrosc.* **1966**, *20* (3), 248−257.
(65) Zeng, W.; Gong, S.; Zhong, C.; Yang, C. Prediction of Oscillator Strength and Transition Dipole Moments With the Nuclear Ensemble Approach for Thermally Activated Delayed Fluorescence Emitters. *J. Phys. Chem. C* **2019**, *123* (15), 10081−10086.
(66) Belay, A. Measurement of Integrated Absorption Cross-Section, Oscillator Strength and Number Density of Caffeine in Coffee Beans by Integrated Absorption Coefficient Technique. *Food Chem.* **2010**, *121* (2), 585−590.
(67) Barnes, N. A.; Godfrey, S. M.; Halton, R. T. A.; Mushtaq, I.; Parsons, S.; Pritchard, R. G.; Sadler, M. A Comparison of the Solid-State Structures of a Series of Phenylseleno-Halogen and Pseudohalogen Compounds, PhSeX (X = Cl, CN, SCN). *Polyhedron* **2007**, *26* (5), 1053−1060.
(68) Shaaban, S.; Negm, A.; Sobh, M. A.; Wessjohann, L. A. Organoselenocyanates and Symmetrical Diselenides Redox Modulators: Design, Synthesis and Biological Evaluation. *Eur. J. Med. Chem.* **2015**, *97* (5), 190−201.
(69) Hoffman, D. J.; Sokolowsky, K. P.; Fayer, M. D. Direct Observation of Dynamic Crossover in Fragile Molecular Glass Formers With 2D IR Vibrational Echo Spectroscopy. *J. Chem. Phys.* **2017**, *146* (12), 124505.

https://doi.org/10.1021/acs.jpcb.1c04939
J. Phys. Chem. B 2021, 125, 8907−8918